INTERNATIONAL JOURNAL OF REFRIGERATION 73 (2017) 24–38

Available online at www.sciencedirect.com

ScienceDirect

journal homepage: www.elsevier.com/locate/ijrefrig

Real-time performance evaluation and potential GHG reduction in refrigerated trailers

F. Bagheri, M.A. Fayazbakhsh, M. Bahrami *

Laboratory for Alternative Energy Conversion (LAEC), School of Mechatronic Systems Engineering, Simon Fraser University, Surrey, BC V3T 0A3, Canada

ARTICLE INFO

Article history:
Received 9 March 2016
Received in revised form 11 August 2016
Accepted 5 September 2016
Available online 12 September 2016

Keywords:
Performance
GHG reduction
Refrigerated trailers
Real-time study

ABSTRACT

In this study, real-time performance of typical refrigerated trailers used in food transportation industry is studied theoretically and experimentally. Two pilot refrigerated trailers are selected and real-time data are collected over different seasons of year 2014–2015 using various measuring equipment during routine operation (fleet dairy distribution reefers) in Vancouver, BC, Canada. A new mathematical model is developed to simulate transient behavior of the on-board vapor compression refrigeration (VCR) systems in trailers and obtain thermal and performance characteristics. The model is validated using the experimental data and executed over the wide periods of measurement. The real-time thermal behavior of the VCR systems is obtained and analyzed. The maximum real-time cooling power and power consumption of the systems are calculated as 17.8 and 18.4 kW. The average yearly energy consumption and COP of the systems are obtained as 11,800 kWh and 0.58, respectively. Tremendous GHG reduction of 8320 kg CO_2 per year per trailer is possible by replacing the current diesel engine-driven VCR systems with battery-powered types.

Évaluation des performances en temps réel et de la réduction potentielle des GES dans les remorques frigorifiques

Mots clés : Performances ; Réduction des GES ; Remorques frigorifiques ; Étude en temps réel

1. Introduction

Despite the immense attention during the past decades, there is a significant potential to reduce energy consumption and greenhouse gas (GHG) emissions from energy systems all around the globe. Based on the fifth report from intergovernmental panel on climate change released in 2013, the average global surface temperature has increased by 0.85 K during 1880–2012 that accelerates the rate of glaciers melting and sea level

* *Corresponding author.* Laboratory for Alternative Energy Conversion (LAEC), School of Mechatronic Systems Engineering, Simon Fraser University, Surrey, BC V3T 0A3, Canada. Fax: +1(778) 782 7514.
E-mail address: mbahrami@sfu.ca (M. Bahrami).
http://dx.doi.org/10.1016/j.ijrefrig.2016.09.008

Nomenclature

$\dot{m}$	mass flow rate $(kg \cdot s^{-1})$
L	length (m)
t	time (s)
u	velocity $(m \cdot s^{-1})$
x	flow direction
α	convection coefficient $(W \cdot m^{-2} \cdot K^{-1})$
Nu	Nusselt number
Pr	Prandtl number
γ	void fraction
η	efficiency
Cp	specific heat capacity $(W \cdot s \cdot kg^{-1} \cdot K^{-1})$
V	compressor displacement $(m^3 \cdot r^{-1})$
C_d	TEV constant

Subscripts/superscripts

i	inside
$cond$	condenser
in	inlet
s	superheated
$2ph$	2-phase
out	outlet
g	gas
c	condensing
a	air
v	volumetric
M	mechanical
e	evaporating
$-$	average value
D	pipe diameter (m)
ρ	density $(kg \cdot m^{-3})$
m	mass (kg)
P	pressure (kPa)
h	enthalpy $(kJ \cdot (kg°C)^{-1})$
T	temperature (K)
Re	Reynolds number
k	thermal conductivity $(W \cdot m^{-1} \cdot K^{-1})$
X	vapor quality
A	area (m^2)
N	compressor rotational speed (rps)
W	power consumption (kW)
B	an arbitrary time-dependent variable
o	outside
ref	refrigerant
$mid1$	boundary of superheated/2-phase regimes
$mid2$	boundary of 2-phase/sub-cooled regimes
l	liquid
tot	total
w	wall
cr	critical
$comp$	compressor
E	electrical
TEV	Thermostatic expansion valve
$evap$	evaporator

rise (WMO and UNEP, 2013; Wu et al., 2013). Among all the energy sectors in the world, the transport sector is responsible for 22% of CO_2 emissions that significantly contributes to global warming (Haass et al., 2015; International Energy Agency, 2013). Around 31% of food supply chain includes refrigerated transportation (Fitzgerald et al., 2011; Jul, 1985). Refrigeration systems consume a tremendous amount of energy leading to large quantities of GHG. Furthermore, about 20% of the total global refrigerant emissions come from mobile air conditioning and refrigeration systems (UNEP, 2010). Transport refrigeration systems operate in a harsh environment and undergo a wide range of cooling demand and constraints imposed by available space and weight. As such, these systems have lower coefficient of performance (COP) than the stationary systems (Tassou et al., 2009).

In addition to the low COP, increasing the quantity of transported goods, home delivery, and expectations on the quality of goods, those bring to increasing the use of refrigerated transport, result in tremendous amount of energy consumption by the refrigerated transport industry (Ahmed et al., 2010; Tassou et al., 2009). Furthermore, the globalized nature of food transportation has caused a long distance transit for many food products (Abban, 2013). In the U.S. alone, it is estimated that processed and fresh food products are transported over 2100 and 2400 km on average, respectively, before being consumed (Abban, 2013; Hill, 2008). In addition, delivery of food products requires frequent door opening that leads to air infiltration and remarkable increase of the cooling demand. It is reported that a food product can be subjected to as many as 50 door-openings during a delivery (James et al., 2006). The low performance combined with harsh operating conditions that lead to significant environmental impacts put an increasing demand on the food industry to find remedies and new solutions for reducing the energy consumption of refrigerated transport (Tassou et al., 2009). There is about 4 million transport refrigerated vehicles in the world, of which about 30% are trailers, 30% are large trucks, and 40% are small trucks and vans (UNEP, 2010). The predominantly used technology in transport refrigeration is vapor compression refrigeration (VCR) (UNEP, 2010). Most of the common VCR systems employed in refrigerated trailers are directly driven by a nearly 2-liter Diesel engines ranging in power from 18 to 30 kW. These diesel engines are run anywhere from 1000 hours to 7200 hours per year depending on type of operation (EPRI, 2010).

Although there are numerous studies in the literature with focus on air conditioning and refrigeration systems in different applications, the number of studies relevant to general category of transport air conditioning and refrigeration systems is restricted (Afram and Janabi-Sharifi, 2014; Anand et al., 2013; Boeng and Melo, 2014; Cho et al., 2013; Defraeye et al., 2015; Ding, 2007; Hermes et al., 2009; Lee and Yoo, 2000; Rodríguez-Bermejo et al., 2007; Sørensen et al., 2015; Spence et al., 2004; Tassou et al., 2009; Tso et al., 2001). Among the studies relevant to transport air conditioning and refrigeration systems, the majority is focused on automotive air conditioning systems (Alkan and Hosoz, 2010; Brown et al., 2002; Cho et al., 2013; Han et al., 2013; Joudi et al., 2003; Tian and Li, 2005; Wang et al., 2005; Yoo and Lee, 2009); however,

Table 1 – Summary of the most relevant existing literature on refrigerated trailers.

Classification	Author	Notes
Thermal study	Jolly et al. (2000).	√ Mathematical modeling of refrigeration unit in a typical electricity-driven reefer. √ Measurements of a few thermal parameters under ambient condition mimicked by an environmental chamber. × Did not study the behavior of COP. × Restricted to steady state condition and full load operation. × Did not consider the effects of door opening, loading/unloading, and transient ambient on the VCR system's behavior.
	Tso et al. (2001).	√ Mathematical modeling of refrigeration unit in a typical electricity-driven reefer. √ Considered effects of hot gas bypass and suction modulation control on performance in partial load. × No experimental data; no model validation. × Restricted to steady state condition. × Did not consider the effects of door opening, loading/unloading, and transient ambient on the VCR system's behavior.
	Moureh and Flick (2004); Moureh et al. (2009).	√ Numerical and experimental study of conditioned air distribution through refrigerated trailers. √ Considered effects of using ducts on air distribution. × No performance evaluation of refrigeration system. × Did not consider the real-time performance and capacity variation of refrigeration system.
	Defraeye et al. (2015).	√ Numerical study on conditioned air distribution through refrigerated trailers. √ Considered effects of food temperature, direction of airflow distribution, spacing between pallets, etc., on food temperature. × No performance evaluation of refrigeration system. × Did not consider the real-time performance and capacity variation of refrigeration system.
	Rodríguez-Bermejo et al. (2007).	√ Experimental study on temperature distribution through refrigerated trailers. √ Considered effects of being loaded or unloaded and thermostat commands on temperature distribution. × No measurements or simulation of VCR system.
Energy efficiency, environmental impacts	Tassou et al. (2009).	√ Estimated average energy intensity, fuel consumption, and CO_2 emission of different food distribution systems in the UK, using statistical and literature data. √ Suggested heat-driven and air-cycle refrigeration systems instead of VCR for food transport and estimated the potential energy saving. × No real-time measurements or modeling for accurate performance investigation of refrigerated vehicles are performed.
	Spence et al (Spence et al., 2004).	√ Designed, built, and tested an air-cycle refrigeration system instead of VCR for food transport to eliminate the direct HFC/HCFC-related environmental impacts. × In general, lower COP and higher fuel-related environmental impact are resulted. × Neither a modeling is performed nor is the transient behavior assessed under real-time condition.
	Sørensen et al. (2015).	√ Developed an MPC (model predictive controller) for refrigeration unit of reefers to increase performance. × Restricted to electrically driven reefers used for sea transportation. × Employed a simplified linear model for thermal behavior of cargo. × No comprehensive model development of refrigeration unit for MPC. × No real-time study of power consumption and performance behavior.

the real-time thermal and performance behavior of the refrigerated trailers have not been studied in depth. Table 1 represents a summary of the pertinent literature on energy efficiency and thermal characteristics of the refrigerated trailers. The tabulated literature review indicates that the pertinent literature lacks the following:

- Real-time investigation of thermal behavior and performance characteristics of refrigerated trailers under different duty cycles.
- Green, sustainable energy solution for current refrigerated trailers and potential GHG reduction.

The present study aims to address the need in the literature by performing a comprehensive theoretical and experimental investigation into typical refrigerated trailers used in the food transportation industry. As such, real-time field data is collected and a new mathematical model is developed for studying the thermal and performance characteristics of such system and evaluating the existing potential GHG reduction.

2. Typical refrigerated trailer for pilot study

Fig. 1 shows two typical refrigerated trailers from food transportation used in this study. These trailers are employed by Saputo Inc. for delivering dairy products. Both trailers are equipped with Diesel engine-driven VCR systems to keep food products cold (4–5 °C set point) during loading and delivery. The studied VCR systems are widely employed in food transportation industries and manufactured by Carrier Transicold. In refrigerated trailer #1, a 4 cylinder, 1.9 liter indirect injection Diesel engine with nominal power of 21.6 kW is employed

(a) Trailer #1; condenser (left), evaporator (right)

(b) Trailer #2; condenser (left), evaporator (right)

Fig. 1 – Examples of typical refrigerated trailers for field data acquisition.

(Carrier Transicold, 2010a). A separate aluminum fuel tank with 190 liter capacity is used to supply the diesel. R-404A is used as the refrigerant in this unit. Based on the manufacturer's catalog, the nominal cooling capacity of the VCR unit is 9.38 and 14.95 kW respectively at evaporator return air temperatures of –18 and 2 °C. The trailer #2 is equipped with a 4 cylinder, 2.2 liter direct injection Diesel engine with 18.5 kW nominal power individually fed from a 190 liter aluminum fuel tank (Carrier Transicold, 2013). The VCR is charged with 7.3 kg of R-404A refrigerant. The condenser and evaporator coils have the dimensions of 1.940 m × 2.176 m × 0.579 m and 1.684 m × 1.149 m × 0.280 m, respectively. Based on the manufacturer's data, the nominal cooling power of VCR is 10.26 and 17.59 kW respectively at evaporator return air temperatures of –18 and 2 °C.

3. Duty cycle definition

Based on the information provided by the local distribution administration and on-site measurements and observations, a duty cycle is defined for the selected trailers. The defined duty cycle is employed to interpret the real-time functionality of the trailers and to analyze the thermal and performance behavior of the VCR system. Figs. 2 and 3 represent samples of the defined duty cycle for trailer #1 respectively for Monday–Wednesday and Saturday–Monday working days. From these figures, one can conclude that for each delivery the VCR system is switched "ON" a while ahead to load the food products. The system stays "ON" for several hours after the loading before the delivery is started to keep the food products in appropriate condition. Due to lack of storage area for the produced goods, the loading is initiated considerably ahead of the delivery. After loading is finished, the trailer is parked exposed to ambient condition (namely sun exposure) for several hours before the delivery. At the end of delivery period, the VCR is switched "OFF" and the trailer is returned back to the parking area.

4. Mathematical model development

In this section, a mathematical model is developed for evaluating the performance of VCR systems under real-time transient operating condition. The complete model includes component sub-models such as: condenser, evaporator, compressor, and expansion valve. The major output parameters from the modeling of a VCR system are cooling power, input power, and coefficient of performance (COP = cooling power/input power).

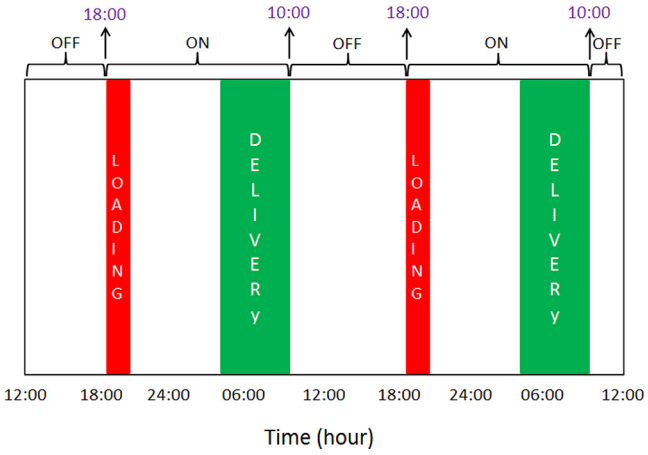

Fig. 2 – Sample obtained duty cycle of VCR unit – Trailer #1, Monday to Wednesday.

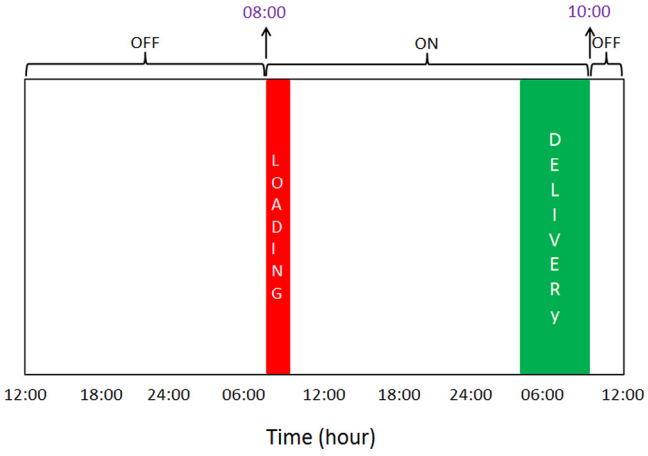

Fig. 3 – Sample obtained duty cycle of VCR unit – Trailer #1, Saturday to Monday.

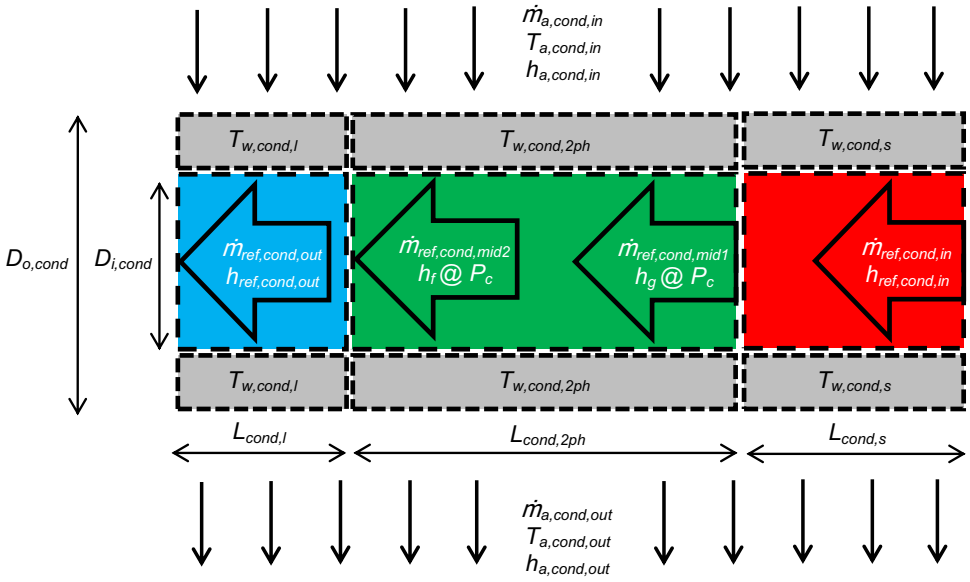

Fig. 4 – Schematic representative of a cross flow condenser in VCR systems (sections from right to left: superheated, 2-phase, sub-cooled).

4.1. *Condenser sub-model*

Conservation of mass, momentum, and energy form a complete mathematical model for the condenser of a VCR system. In general, three different refrigerant regimes may exist in a condenser including: superheated, 2-phase, and sub-cooled; thus, the governing equations are written separately for each of these regimes. Following Li and Alleyne (2010) and Liang et al. (2010), a schematic representative of the heat transfer regimes in a condenser is shown in Fig. 4.

- Conservation of mass for refrigerant in superheated section (integrated over volume):

$$\dot{m}_{ref,cond,in} - \dot{m}_{ref,cond,mid1} = \frac{\pi}{4} D_{i,cond}^2 \left(L_{cond,s} \frac{\partial \bar{\rho}_{ref,cond,s}}{\partial t} + \bar{\rho}_{ref,cond,s} \frac{\partial L_{cond,s}}{\partial t} \right) \tag{1}$$

- Conservation of mass for refrigerant in 2-phase section:

$$\dot{m}_{ref,cond,mid1} - \dot{m}_{ref,cond,mid2} = \frac{\pi}{4} D_{i,cond}^2 \left(L_{cond,2ph} \frac{\partial \bar{\rho}_{ref,cond,2ph}}{\partial t} + \bar{\rho}_{ref,cond,2ph} \frac{\partial L_{cond,2ph}}{\partial t} \right) \tag{2}$$

- Conservation of mass for refrigerant in sub-cooled (liquid) section (integrated over volume):

$$\dot{m}_{ref,cond,mid2} - \dot{m}_{ref,cond,out} = \frac{\pi}{4} D_{i,cond}^2 \left(L_{cond,l} \frac{\partial \bar{\rho}_{ref,cond,l}}{\partial t} + \bar{\rho}_{ref,cond,l} \frac{\partial L_{cond,l}}{\partial t} \right) \tag{3}$$

- Conservation of momentum for refrigerant (fully-developed flow, integrated over volume):

$$\frac{\partial (mu)_{cond}}{\partial t} = \dot{m}_{ref,cond,in} \left(\frac{\dot{m}_{ref,cond,in}}{\rho_{ref,cond,in} \frac{\pi}{4} D_{i,cond}^2} \right) - \dot{m}_{ref,cond,out} \left(\frac{\dot{m}_{ref,cond,out}}{\rho_{ref,cond,out} \frac{\pi}{4} D_{i,cond}^2} \right) - \frac{\partial P}{\partial x} \left(\frac{\pi}{4} D_{i,cond}^2 L_{cond,tot} \right) + \text{Viscous losses} \tag{4}$$

- Conservation of energy for refrigerant in superheated section:

$$(\dot{m}h)_{ref,cond,in} - \dot{m}_{ref,cond,mid1} h_g - \pi D_{i,cond} L_{cond,s} \alpha_{ref,cond,s} \left(\bar{T}_{ref,cond,s} - \bar{T}_{w,cond,s} \right) = \frac{\pi}{4} D_{i,cond}^2 \left(L_{cond,s} \bar{h}_{ref,cond,s} \frac{\partial \bar{\rho}_{ref,cond,s}}{\partial t} + \bar{\rho}_{ref,cond,s} \bar{h}_{ref,cond,s} \frac{\partial L_{cond,s}}{\partial t} + \bar{\rho}_{ref,cond,s} L_{cond,s} \frac{\partial \bar{h}_{ref,cond,s}}{\partial t} \right) \tag{5}$$

where the convective heat transfer coefficient $\alpha_{ref,cond,s}$ is calculable using Dittus-Boelter correlation (Liang et al., 2010; Shah and Sekulic, 2003; see Eq. (6)). The left hand side of the above energy equation represents the net rate of energy entering the superheated region via convection and conduction. The right hand side represents the rate of variations of total energy in the superheated region. The length of superheated region and the enthalpy and density of refrigerant can change by time and are appeared on the right hand side.

$$Nu = \frac{\alpha_{ref,cond,s} D_{i,cond}}{\bar{k}_{ref,cond,s}} = 0.023 \mathrm{Re}^{0.8} \mathrm{Pr}^{0.4} \tag{6}$$

- Conservation of energy for refrigerant in 2-phase section:

$$\dot{m}_{ref,cond,mid1} h_g - \dot{m}_{ref,cond,mid2} h_l - \pi D_{i,cond} L_{cond,2ph} \alpha_{ref,cond,2ph} \left(T_c - \bar{T}_{w,cond,2ph} \right) = \frac{\pi}{4} D_{i,cond}^2 \left(L_{cond,2ph} \frac{\partial \left(\overline{\rho h} \right)_{ref,cond,2ph}}{\partial t} + \left(\overline{\rho h} \right)_{ref,cond,2ph} \frac{\partial L_{cond,2ph}}{\partial t} \right) \tag{7}$$

The following correlations also govern the 2-phase region (Wang et al., 2007):

$$\left(\overline{\rho h}\right)_{ref,cond,2ph} = \left(\rho_g h_g \gamma + \rho_l h_l (1-\gamma)\right)_{cond} \tag{8}$$

$$\gamma = \frac{1}{1+\frac{1-X}{X}\left(\frac{\rho_g}{\rho_l}\right)^{\frac{2}{3}}} \tag{9}$$

Also, the convective heat transfer coefficient $\alpha_{ref,cond,2ph}$ is calculated from Kandlikar correlation (Beatty and Katz, 1948; Browne and Bansal, 2002):

$$\alpha_{ref,cond,2ph} = 0.023\,\mathrm{Re}_{l,cond}^{0.8}\,\mathrm{Pr}_{l,cond}^{0.4}\,\frac{k_{l,cond}}{D_{i,cond}}\left[(1-X)^{0.8} + \frac{3.8X^{0.76}(1-X)^{0.04}}{\left(P_c/P_{cr}\right)^{0.38}}\right] \tag{10}$$

- Conservation of energy for refrigerant in sub-cooled (liquid) section:

$$\begin{aligned}&\dot{m}_{ref,cond,mid2}h_l - (\dot{m}h)_{ref,cond,out} - \pi D_{i,cond}L_{cond,l}\alpha_{ref,cond,l}\left(\overline{T}_{ref,cond,l} - \overline{T}_{w,cond,l}\right)\\ &= \frac{\pi}{4}D_{i,cond}^2\left(L_{cond,l}\overline{h}_{ref,cond,l}\frac{\partial\overline{\rho}_{ref,cond,l}}{\partial t} + \overline{\rho}_{ref,cond,l}\overline{h}_{ref,cond,l}\frac{\partial L_{cond,l}}{\partial t} + \overline{\rho}_{ref,cond,l}L_{cond,l}\frac{\partial\overline{h}_{ref,cond,l}}{\partial t}\right)\end{aligned} \tag{11}$$

- Conservation of energy for wall in superheated section:

$$\begin{aligned}&\pi D_{i,cond}L_{cond,s}\alpha_{ref,cond,s}\left(\overline{T}_{ref,cond,s} - \overline{T}_{w,cond,s}\right)\\ &- \alpha_{a,cond}\left(\pi D_{o,cond}L_{cond,s} + \eta_{fin}A_{fin,s}\right)\left(\overline{T}_{w,cond,s} - \overline{T}_{a,cond}\right)\\ &= \frac{\pi}{4}\left(D_{o,cond}^2 - D_{i,cond}^2\right)\left[L_{cond,s}(\rho Cp)_w\frac{\partial\left(\overline{T}_{w,cond,s}\right)}{\partial t} + (\rho Cp)_w\overline{T}_{w,cond,s}\frac{\partial L_{cond,s}}{\partial t}\right]\end{aligned} \tag{12}$$

- Conservation of energy for wall in 2-phase section:

$$\begin{aligned}&\pi D_{i,cond}L_{cond,2ph}\alpha_{ref,cond,2ph}\left(T_c - \overline{T}_{w,cond,2ph}\right)\\ &- \alpha_{a,cond}\left(\pi D_{o,cond}L_{cond,2ph} + \eta_{fin}A_{fin,2ph}\right)\left(\overline{T}_{w,cond,2ph} - \overline{T}_{a,cond}\right)\\ &= \frac{\pi}{4}\left(D_{o,cond}^2 - D_{i,cond}^2\right)\left[L_{cond,2ph}(\rho Cp)_w\frac{\partial\left(\overline{T}_{w,cond,2ph}\right)}{\partial t} + (\rho Cp)_w\overline{T}_{w,cond,2ph}\frac{\partial L_{cond,2ph}}{\partial t}\right]\end{aligned} \tag{13}$$

- Conservation of energy for wall in sub-cooled (liquid) section:

$$\begin{aligned}&\pi D_{i,cond}L_{cond,l}\alpha_{ref,cond,l}\left(\overline{T}_{ref,cond,l} - \overline{T}_{w,cond,l}\right)\\ &- \alpha_{a,cond}\left(\pi D_{o,cond}L_{cond,l} + \eta_{fin}A_{fin,l}\right)\left(\overline{T}_{w,cond,l} - \overline{T}_{a,cond}\right)\\ &= \frac{\pi}{4}\left(D_{o,cond}^2 - D_{i,cond}^2\right)\left[L_{cond,l}(\rho Cp)_w\frac{\partial\left(\overline{T}_{w,cond,l}\right)}{\partial t} + (\rho Cp)_w\overline{T}_{w,cond,l}\frac{\partial L_{cond,l}}{\partial t}\right]\end{aligned} \tag{14}$$

- Conservation of energy for air:

$$\begin{aligned}&\dot{m}_{a,cond}\left(h_{a,cond,in} - h_{a,cond,out}\right)\\ &= \alpha_{a,cond}\left(\pi D_{o,cond}L_{cond,tot} + \eta_{fin}A_{fin}\right)\left(\overline{T}_{a,cond} - \overline{T}_{w,cond}\right)\end{aligned} \tag{15}$$

where:

$$\overline{T}_{w,cond} = \frac{\overline{T}_{w,cond,s}L_{cond,s} + \overline{T}_{w,cond,2ph}L_{cond,2ph} + \overline{T}_{w,cond,l}L_{cond,l}}{L_{cond,tot}} \tag{16}$$

4.2. Evaporator sub-model

Similar to the condenser, writing the conservation of mass, momentum, and energy forms a complete model for evaporator in a VCR system. It should be noted that there are only two sections in an evaporator: 1) 2-phase, and 2) superheated.

4.3. Compressor sub-model

For a compressor in VCR systems, the refrigerant mass flow rate can be obtained from the following correlation (Koury et al., 2001):

$$\dot{m}_{ref,comp} = NV\rho_{ref,comp,in}\eta_v \tag{17}$$

where volumetric efficiency η_V is a function of evaporating and condensing pressures. Also, the power input to compressor can be calculated using the following equation:

$$W_{comp} = \frac{\dot{m}_{ref,comp}\left(h_{ref,comp,out} - h_{ref,comp,in}\right)}{\eta_E\eta_M} \tag{18}$$

4.4. Expansion valve

Assuming an isenthalpic process, the following correlations can be utilized for modeling the expansion valve behavior (Liang et al., 2010):

$$\dot{m}_{ref,TEV} = C_d A\sqrt{\rho_{ref,TEV,in}\left(P_c - P_e\right)} \tag{19}$$

$$h_{ref,TEV,in} = h_{ref,TEV,out} \tag{20}$$

4.5. Unknowns of the model

Based on the obtained equations of the mathematical model, a number of unknowns are calculable after the solution. All the time-gradient terms appeared in the equations are discretized using the finite difference approach. As such, the following equation is used for an arbitrary variable B:

$$\frac{\partial B}{\partial t} = \frac{B_{n+1} - B_n}{\Delta t} \tag{21}$$

Accordingly, the transient solution is commenced with an initial condition (@ $n = 0$) and marches through time by solving all the equations at each time step. The model obtained can be written as a set of 26 non-linear equations with 26 unknowns presented in Table 2. The calculated values from each

Table 2 – Calculated parameters at each time step.

$\dot{m}_{ref,cond,in}$ $(\dot{m}_{ref,evap,out}), (\dot{m}_{ref,comp})$	$\dot{m}_{ref,cond,out}$ $(\dot{m}_{ref,evap,in}), (\dot{m}_{ref,TEV})$	$h_{ref,cond,in}$ $(h_{ref,comp,out})$	$h_{ref,cond,out}$ $h_{ref,TEV,in}$
$\dot{m}_{ref,evap,mid}$	$L_{cond,s}$	$\dot{m}_{ref,cond,mid1}$	$\dot{m}_{ref,cond,mid2}$
$L_{evap,2ph}$	$L_{evap,s}$	$L_{cond,2ph}$	$L_{cond,l}$
$h_{ref,evap,in}$	$h_{ref,evap,out}$	P_e	P_c
$(h_{ref,TEV,out})$	$(h_{ref,comp,in})$	(T_e)	(T_c)
$T_{w,cond,s}$	$T_{w,cond,2ph}$	$T_{w,cond,l}$	$T_{w,evap,s}$
$T_{w,evap,2ph}$	$T_{a,cond,out}$	$T_{a,evap,out}$	γ_{cond}
	γ_{evap}	W_{comp}	

time step are used as known for the next time step. A Newton-Raphson based solver is developed in C for numerical solution of the equations set.

5. Experimental setup for field data acquisition

A major challenge of this study has been to obtain field data from the pilot refrigerated trailers under realistic operational conditions. The challenge of data acquisition from a moving trailer that is frequently loaded and unloaded is solved using specific types of data loggers equipped with internal memories. Figs. 5 and 6 show samples of the installed data loggers on the VCR system. Using the installed equipment, temperature, humidity and air velocity are measured at different spots on the VCR system every 10 seconds. The data have been collected on-board the refrigerated trailers for several months during warm and mild seasons of the year 2014–2015. A number of 4 Rotronic temperature and humidity sensors model HC2-S3 with accuracy of ±0.1 °C and ±0.5% RH, 2 MicroDAQ temperature and humidity data-loggers model RFID with accuracy of ±0.5 °C and ±2% RH, and 2 EXTECH 4-channel data-logging thermometers with accuracy of ±0.1 °C are utilized for the measurements.

The accuracy of utilized air velocity sensors used for the evaporator and condenser flow measurements is ±0.15 $m.s^{-1}$. The fuel consumption of trailer is measured by accurately filling the fuel tank during the periods of measurement. As such, the total fuel consumption for each period is obtained by adding the amount of fuel refills during that period.

6. Results and discussion

The field data are acquired during warm and mild seasons of the year 2014–2015 to cover a wide range of operational conditions in Vancouver, BC, Canada. The mathematical model is also executed to simulate the thermal and performance characteristics of the VCR system under different operating conditions.

6.1. *Field data acquisition*

The measurements are performed on the pilot trailers to obtain the real-time thermal behavior of the VCR systems. Figs. 7–10 show samples of the acquired data from measurements. The following can be concluded from these results:

- The ambient temperature varies remarkably during day and night (see Fig. 7) that imposes variable cooling load and operational condition on the VCR system. This is noteworthy, since the measurements are conducted in Vancouver, BC, Canada which has a mild climate. Such variation could be more pronounced in other geographical locations. Due to heat gain from trailer wall and air infiltrations during food

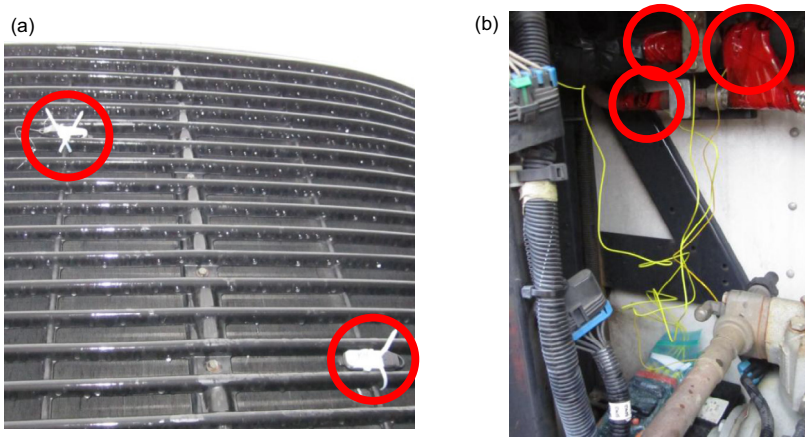

Fig. 5 – Sample installed measuring equipment on the condensing unit, (a) air temperature and humidity at condenser inlet, (b) refrigerant temperature at compressor inlet and outlet.

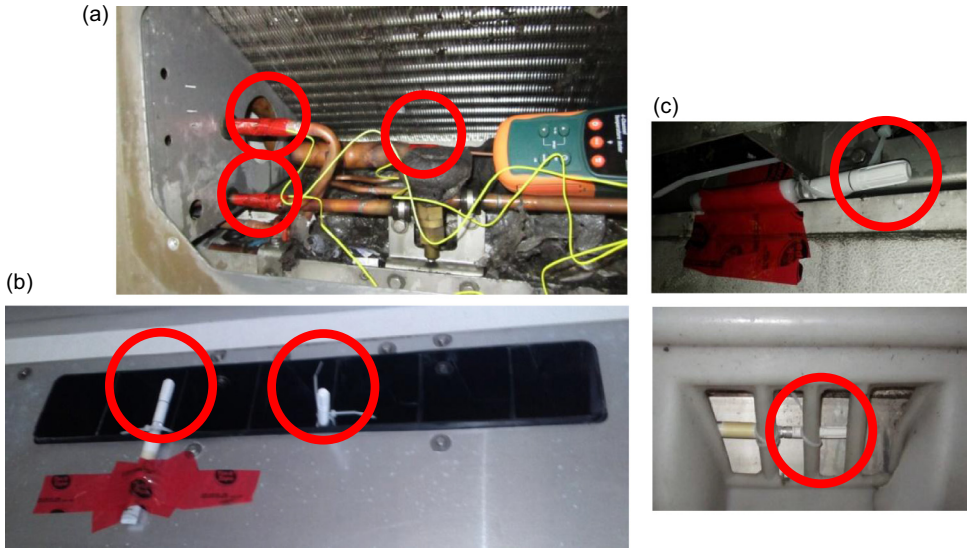

Fig. 6 – Sample installed measuring equipment on the evaporating unit; (a) refrigerant temperature at evaporator coil inlet and outlet; air temperature and humidity at (b) evaporator outlet, (c) evaporator inlet.

load/unload, the refrigeration unit frequently turns on-off during "ON" periods (see Fig. 8) to keep the indoor temperature close to a pre-set desired temperature (~4 °C). The loaded food products do not impose any additional cooling loads on the VCR system because they have already been cooled down to desired temperature before being loaded. The refrigerant temperature during day and night is a function of duty cycle and ambient temperature variations.

- The frequency of VCR on–off cycling right after switching the system "ON" from an "OFF" condition is higher than usual (see Figs. 8–10). Specially, whenever the system is switched "ON" after a longer "OFF" period, the intensity of on–off cycling is more significant. This higher rate of fluctuations happens due to thermal inertia of the trailer compartment. During the "OFF" periods, heat is stored throughout the thermal mass (walls) of the trailer. As such, the VCR system must work harder to overcome the thermal inertia and keep the temperature desirable, which leads to more intensive fluctuations and higher energy consumption.
- At the end of each "ON" period that coincides with delivery hours, some irregular fluctuations with larger amplitudes can be observed on the evaporator air temperature graphs (see Figs. 9 and 10). This chaotic behavior of the air temperature emerges due to frequent door opening for unloading products that causes ambient air infiltration into the trailer. The door openings and high-amplitude temperature fluctuations during the delivery hours not even impose extra cooling load on the VCR unit, but also destructively affect the quality of food products.
- Loading the food products several hours earlier than the delivery leaves a loaded trailer in the parking area exposed to ambient temperature and sometimes sun radiation that leads to significant energy losses due to inefficient insulation of trailer walls. The frequent on–off cycling of the VCR unit during these periods (see Fig. 8), specially Sundays for trailer #1 (see Fig. 10) and most of weekdays for trailer #2, indicates the enormity of such heat gain and the corresponding energy losses.

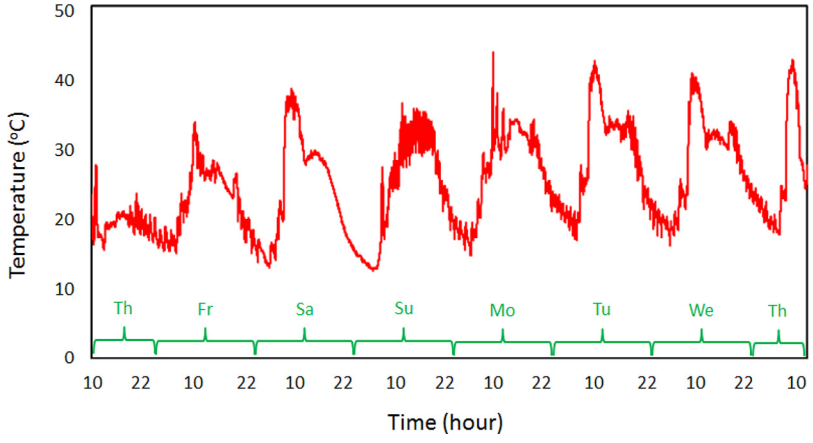

Fig. 7 – Sample measured ambient air (condenser inlet) temperature – July.

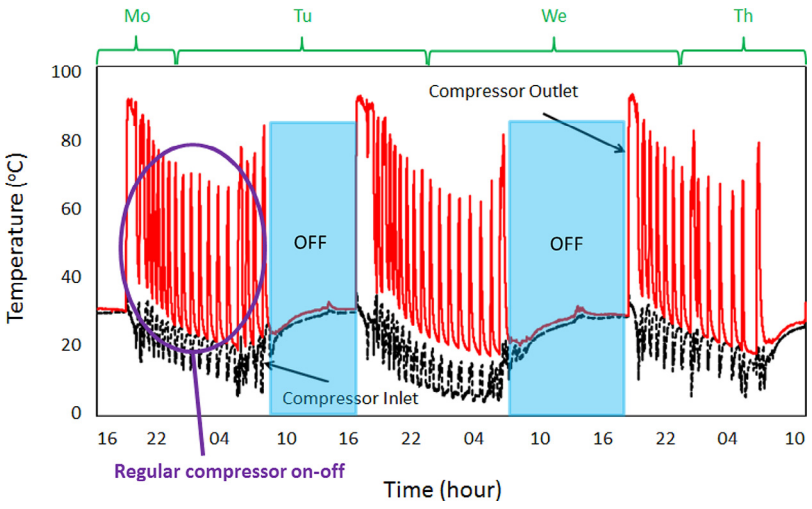

Fig. 8 – Sample measured refrigerant temperature variations at compressor inlet and outlet – Trailer #1, Mon to Thu, July.

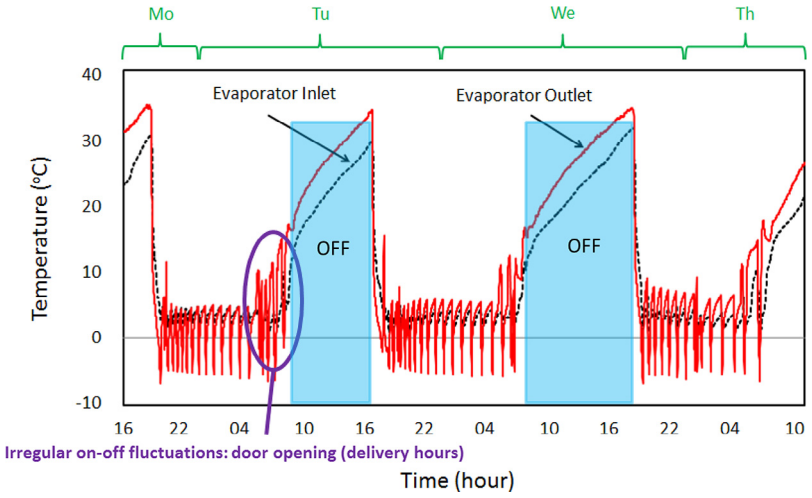

Fig. 9 – Sample measured air temperature variations at evaporator inlet and outlet – Trailer #1, Mon to Thu, July.

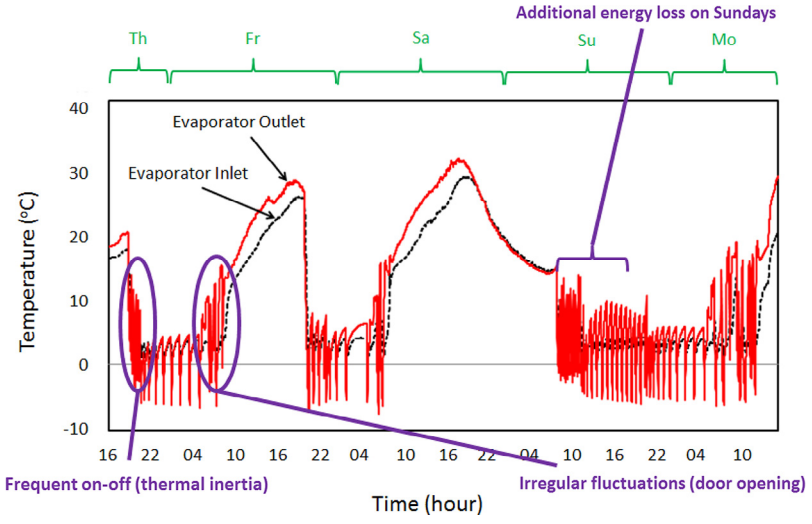

Fig. 10 – Sample measured air temperature variations at evaporator inlet and outlet – Trailer #1, Thu to Mon, July.

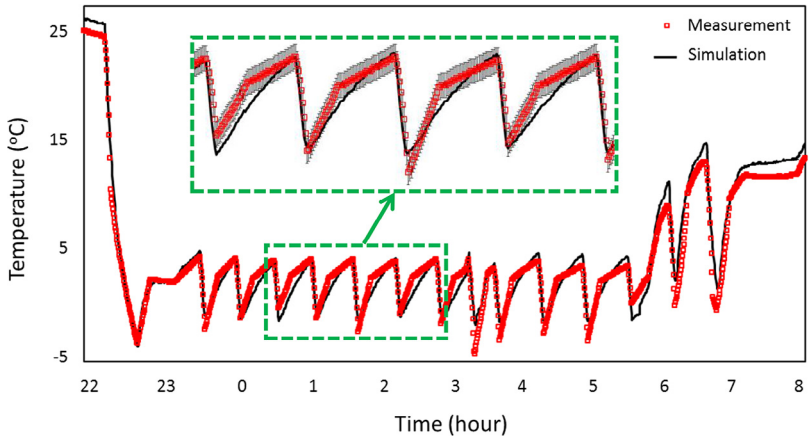

Fig. 11 – Sample simulated and measured air temperature at evaporator outlet – Trailer #2, Wed to Thu, August.

6.2. *Model verification and simulation results*

The developed mathematical model is employed for performance investigation of the pilot trailers under realistic working conditions. The required physical parameters of the VCR system are obtained from manufacturer's data and on-site measurements and inputted into the model. The model is then executed over the measurement periods and its outputs are compared with our measurements; the comparison shows a good agreement between the results. Two sample comparisons of the modeling results with field data are presented in Figs. 11 and 12. The temperature of the cold air leaving the evaporator and the instantaneous cooling power delivered by the VCR system are compared on these graphs. In Fig. 13 also a zoomed-in comparison between model and measurements of cooling power during a typical "ON" period is shown. The instantaneous cooling power from measurements (Figs. 12 and 13) is directly calculated from air enthalpy entering and leaving the evaporator (obtained from psychrometric chart calculations based on the measured temperature and humidity) and the air velocity data (obtained from air velocity sensors). The comparisons show a maximum relative difference of 8.5% between the model and measurement results. The uncertainty analysis of the experimental data shows a maximum uncertainty of ±0.5 °C for the measured temperature and 2.0% for the measured cooling power values.

Figs. 11 and 12 show the fluctuations of the conditioned air temperature and cooling power during the regular and chaotic on–off cycling. The previously described behavioral characteristics of air-side temperature in the last section can be observed in Fig. 11. From Fig. 12 one can conclude that at the beginning of each "ON" period as well as during the delivery hours (end of each operating cycle) the cooling power of the VCR system is higher. This increase is due to thermal inertia of the trailer (at beginning) and ambient air infiltration (during delivery) that impose a higher cooling demand on the VCR system. The simulation and measurements over the study periods show that the maximum delivered cooling power by the VCR system of trailers #1 and #2 are 16.9 and 17.8 kW that happens at 19:50 and 18:47 of a warm day in August, respectively.

One of the major sough-after outcomes of this study is the real-time COP calculation of the VCR system. To obtain the real-

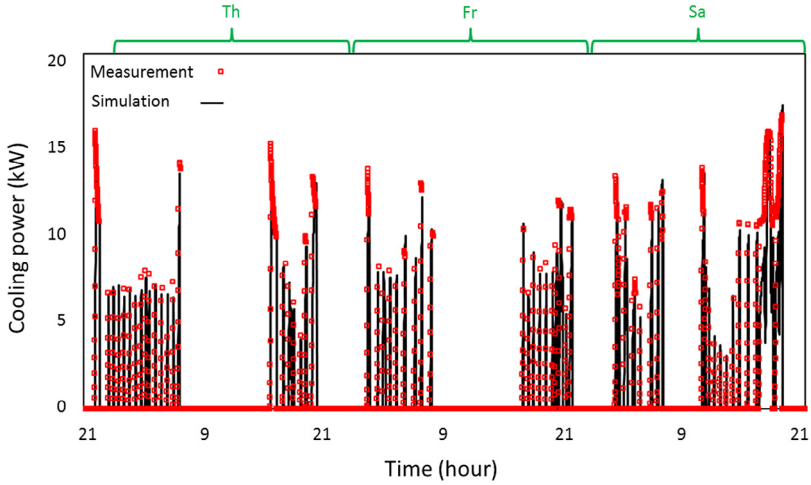

Fig. 12 – Sample simulated and measured cooling power – Trailer #2, Thu to Sat, August.

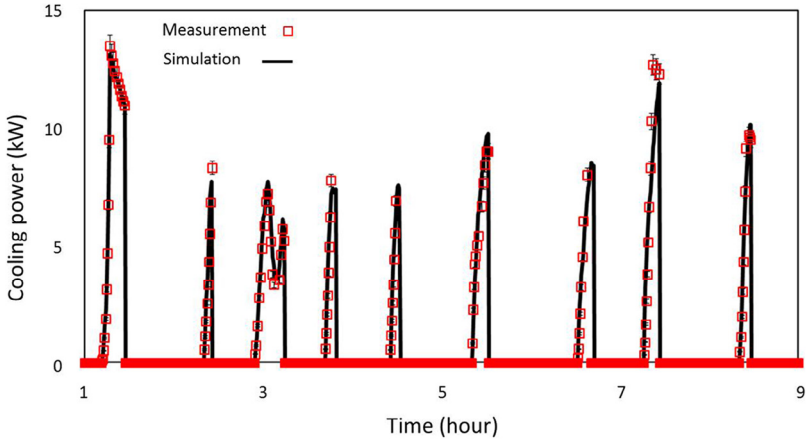

Fig. 13 – Sample zoomed simulated and measured cooling power – Trailer #2, Friday morning, August.

time COP, both instantaneous cooling power and input power to the VCR system are required. Because the VCR system is directly driven by a Diesel engine, the instantaneous mechanical power input to the compressor and fans of the system cannot be directly measured due to many challenges of which the movement of trailer is the most important one. As such, the only way of obtaining the instantaneous power consumption and COP is through the simulation using the developed and verified model. However, the measurement of overall energy consumption by the refrigerated trailer is also conducted over the study period to achieve comprehensive and more reliable results.

The most detailed overall energy consumption measured in this study is the amount of fuel refill of the trailer tank in different intervals. To achieve the highest accuracy of the fuel consumption data, the fuel tank is fully filled at each refill and thus, the amount of fuel consumption during each interval is equal to the amount of fuel refill corresponding to that interval. Fig. 14 shows a sample of simulated transient power input to VCR system over a 10-day period, August 2015, Greater Vancouver, BC, Canada. Based on the transient simulation results over day and nights of mild and warm seasons, the power consumption of the VCR system (trailer #2) varies between 11.2 and 18.4 kW over the "ON" cycles depending upon the imposed cooling load as well as the ambient and indoor temperatures. As expected, the power consumption of the VCR system is higher at the beginning and end of each "ON" cycle due to higher imposed cooling load respectively because of thermal inertia and door opening during the delivery. Based on the simulations over the year 2015, the maximum power consumption by the VCR system of trailers #1 and #2 are 18.0 and 18.4 kW that appear at 18:02 on August 6 and 17:36 on July 28, Greater Vancouver, BC, Canada, respectively. Furthermore, the average power consumption over an "ON" cycle is higher in days of the warm seasons and lower during nights of mild seasons. Based on the obtained results, the maximum power consumption of the studied VCR systems of the trailers during a complete "ON" cycle is 44.5 kWh that occurs in a warm day of August. The average yearly energy consumption of the simulated VCR systems is 11,800 kWh.

Eventually, the real-time COP of the refrigerated trailers is obtained using the simulated transient cooling power and power consumption over the study period. Fig. 15 shows a sample of the obtained COP results. Based on all the obtained results

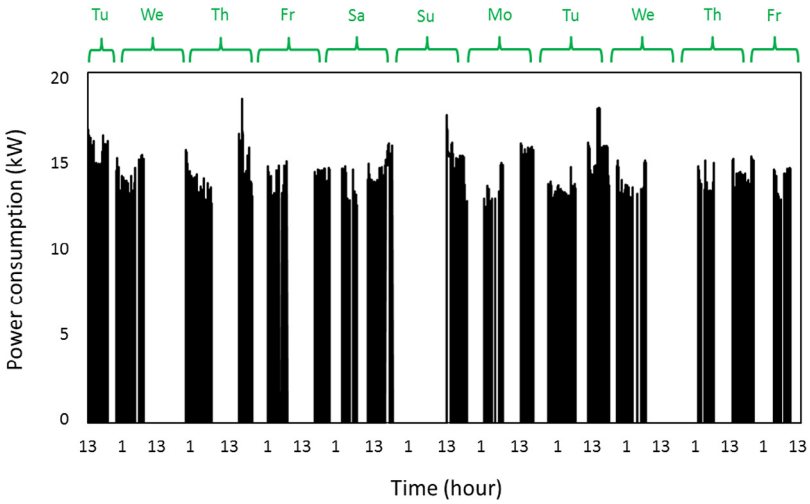

Fig. 14 – Sample simulated power consumption for 10 days – Trailer #2, August.

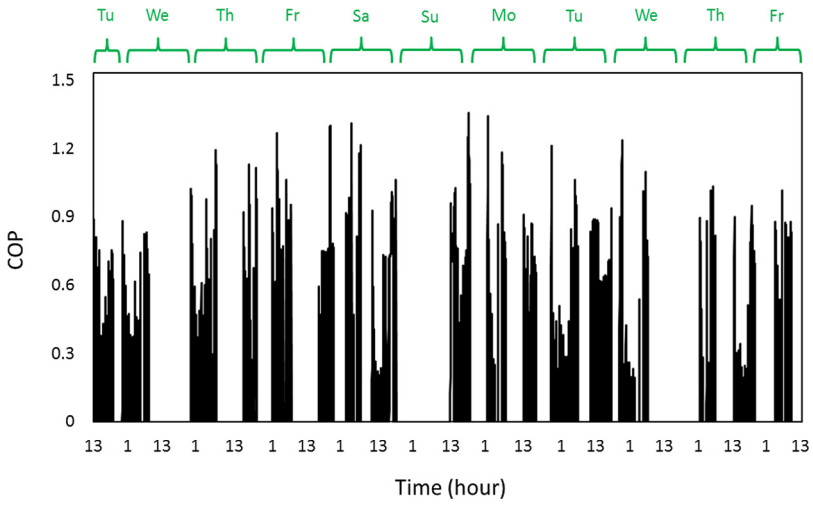

Fig. 15 – Sample simulated COP for 10 days – Trailer #2, August.

during mild and warm seasons for both trailers, the following can be concluded:

- The real-time COP of the refrigerated trailers varies in a range of 0.001–1.33 over the "ON" periods. This wide range of COP indicates sensitivity of the VCR systems to the operating conditions. The significantly small values of COP (less than 0.1) exist over a short period of time at most of the on–off fluctuations right after the VCR starts working. Over such periods, the VCR immediately starts consuming significant power; however, it takes time (several seconds up to one-two minutes) to deliver a considerable cooling effect.
- The larger COP values appear during the beginning and final hours of most "ON" periods although the power consumption is a bit higher over those hours (see Fig. 14). These higher COP values exist due to higher cooling power of the VCR system over those hours (see Fig. 12). However, in the middle of most "ON" periods the COP is smaller due to smaller cooling power although the power consumption is also a bit lower (see Figs. 12 and 14).
- The average simulated COP of the trailers over the year is 0.58. This number is significantly smaller than the COP of stationary systems, usually larger than 3 (Alklaibi, 2008; Macagnan et al., 2013; Park and Jung, 2007; Wang et al., 2005), which highlights the importance of studying the food transportation industry due to enormous global energy consumption and environmental impacts.
- Using the measured fuel consumption of the trailer, the experimental COP is also calculated. As such, the measured cooling power is integrated over time and used along with the measured fuel consumption over the same period of time, which returns a magnitude of 0.185 as an overall time-averaged COP for the engine-VCR combination. Based on the manufacturer's data, the average thermal efficiency of the employed Diesel engines is nearly 30% (Carrier Transicold, 2012; Li et al., 2016; Rapalis and Skac, 2015). As such, the time-averaged COP of the VCR systems will be 0.62 based on the measurements. Accordingly, there is only 6.5% relative difference between the simulated and measured average COP values of the studied VCR systems that verifies a good accuracy of the obtained results.

6.3. *Potential GHG reduction from refrigerated trailers*

The obtained results from simulations and measurements show that a typical VCR of a refrigerated trailer that works in a mild climatic condition (Vancouver, British Columbia, Canada) consumes 11,800 kWh per year. As such, assuming an average Diesel engine's thermal efficiency of 30%, the typical refrigerated trailer consumes more than 3000 liter per year of Diesel fuel. The maximum required power and energy during an "ON" period throughout the year (including loading and delivery) are calculated as 18.4 kW and 44.5 kWh, respectively. Based on the obtained data from GPS of the trucks that move the studied trailers, more than 60,000 km per year is travelled by each trailer. Therefore, a heavy and low efficiency engine-driven VCR (total of 1100 kg including the fuel tank) is transported more than 60,000 km per year that significantly contributes to GHG emissions. As a key conclusion of this study regarding the required power and energy and performance variations of the VCR systems, it is highly recommended that the engine-driven refrigerated trailers are replaced by battery-powered refrigerated trailers to eliminate the relevant GHG emissions. The proposed battery-powered VCR may not be applicable to all reefer trucks, certainly for inter-city and long-haul vehicles, battery powered VCR may be a challenging solution, especially considering battery charging time and infrastructure needed. However; for fleet reefer trucks, it is a viable and clean solution. Based on the manufacturer's data (Carrier Transicold, 2010b, 2012), eliminating the engine and fuel tank will reduce up to 600 kg of the total trailer's weight. Assuming an average specific power and energy of 300 $W.kg^{-1}$ and 0.2 $kWh.kg^{-1}$ for Li-ion batteries to replace the engine and fuel tank (Brodd, 2012; Tahil, 2010), the maximum weight of required batteries will be 225 kg. Thus, 375 kg of total trailer's weight can be reduced by replacing the engine-driven VCR with a battery-driven VCR system. This weight reduction equals 1.5% of total truck-full

trailer weight based on the field measurements and manufacturer's data.

Utilizing the available data on average fuel consumption versus weight of freight in transportation industry, more than 0.5% of total fuel consumption by the truck that moves the trailer will be reduced as a result of such weight reduction (Casadei and Broda, 2008; Galos et al., 2015). Thus, assuming an average truck-trailer fuel consumption of 35 L per 100 km (Garthwaite, 2012; Natural Resources Canada, 2016), at least 105 liters of Diesel fuel can be saved per year per truck-trailer. In addition, all the fuel consumption (3000 liter per year based on the obtained results) and GHG emissions from the refrigerated trailer's Diesel engine will be eliminated. As such, a total of 3105 liters of Diesel fuel that is equivalent to 8320 kg CO_2 per year (U.S. Energy Information Administration, 2016) can be reduced per truck-trailer by replacing the engine-driven VCR with battery-powered type. In many areas around the globe, electricity is produced using clean technologies such as hydro, wind, and solar energy. Eventually, if all the engine-driven trailers in the world (estimated to be 1.2 million (UNEP, 2010)) are replaced by battery-powered types feed from clean tech-generated electricity, more than 3.7 billion liters of Diesel fuel will be saved and up to 10 million tons of CO_2 can be reduced annually.

7. Conclusions

This paper presented a mathematical and experimental investigation into real-time performance of typical refrigerated trailers and estimated potential energy saving and GHG reduction. Two typical refrigerated trailers were selected for the study. These trailers were employed for daily-based food delivery in Vancouver, British Columbia, Canada. A number of temperature, humidity, and air velocity measuring equipment were installed on the VCR units to obtain real-time field data in mild and warm seasons of the year. In addition, the duty cycle, manifest, truck and trailer fueling, and GPS data were acquired from the user and on-site measurements. A new mathematical model, which simulated transient thermodynamic and heat transfer characteristics of the VCR systems, was developed and validated using the real-time data. The followings were concluded from the mathematical and experimental study:

- Three different regimes of inefficient on–off cycling by VCR system were observed: 1) a high frequency fluctuation regime due to high cooling demand as a result of thermal inertia of trailer immediately after starting the VCR from "OFF" period, 2) a frequent regular fluctuation regime to keep the food product at the desired temperature, 3) an irregular fluctuation regime at the end of each "ON" period due to ambient air infiltration as a result of door openings during food delivery.
- The maximum delivered cooling power by the VCR system of the studied trailers #1 and #2 were obtained as 16.9 and 17.8 kW that happened in the afternoon of warm days in August. The maximum power consumption by the VCR system of trailers #1 and #2 were 18.0 and 18.4 kW that appeared in the afternoon of warm days of August. The maximum total energy consumption of the VCR systems during a complete "ON" period was 44.5 kWh occurring in a warm day of August. The average yearly energy consumption of the VCR systems was 11,800 kWh.
- The real-time COP of the refrigerated trailers was obtained that showed a range of 0.001–1.33 over the "ON" periods. The yearly-averaged simulated and measured COP of the trailers was 0.58 and 0.62, respectively.
- It was recommended that the engine-driven VCR systems would be replaced by battery-powered VCR systems to reduce the weight and GHG emissions. It was calculated that a total of 375 kg per trailer can be reduced by this replacement that contributes to 0.5% reduction in GHG by the truck's engine. In total, an amount of 3105 liters of Diesel fuel from both the truck and trailer equivalent to 8,320 kg CO_2 per year emission can be reduced by this replacement. Expanding the obtained results to all the refrigerated trailers in the world showed that there is a potential reduction of 3.7 billion liters of Diesel fuel and 10 million tons of CO_2 per year by this replacement.

Acknowledgments

This work was supported by Automotive Partnership Canada (APC), Grant No. APCPJ 401826-10. The authors would like to thank kind support from Saputo Inc., Burnaby, BC, Canada. The authors also would like to thank assistance from Dr. Wendell Huttema (laboratory engineers at *LAEC*), Mr. Marius Haiducu (laboratory manager of *LAEC*), Mr. Jordan Lam (Co-op student at *LAEC*), Mr. Jit Tian Lim (Co-op student at *LAEC*), and Mr. Tian Lin Yang (Co-op student at *LAEC*) during the measurements and data acquisition.

REFERENCES

Abban, S., Microbial behaviour and cross contamination between cargoes in containerized transportation of food, University of Copenhagen, 2013.

Afram, A., Janabi-Sharifi, F., 2014. Review of modeling methods for HVAC systems. Appl. Therm. Eng. 67, 507–519.

Ahmed, M., Meade, O., Medina, M.A., 2010. Reducing heat transfer across the insulated walls of refrigerated truck trailers by the application of phase change materials. Energy Convers. Manag. 51, 383–392.

Alkan, A., Hosoz, M., 2010. Comparative performance of an automotive air conditioning system using fixed and variable capacity compressors. Int. J. Refrigeration 33, 487–495.

Alklaibi, A.M., 2008. Evaluating the possible configurations of incorporating the loop heat pipe into the air-conditioning systems. Int. J. Refrigeration 31, 807–815.

Anand, S., Gupta, A., Tyagi, S.K., 2013. Simulation studies of refrigeration cycles: a review. Renew. Sustain. Energy Rev. 17, 260–277.

Beatty, K., Katz, D., 1948. Condensation of vapours on the outside of finned tube. Chem. Eng. Prog. 44, 55–70.

Boeng, J., Melo, C., 2014. Mapping the energy consumption of household refrigerators by varying the refrigerant charge and the expansion restriction. Int. J. Refrigeration 41, 37–44.

Brodd, R.J., 2012. Batteries for Sustainability. Springer.
Brown, J.S., Yana-Motta, S.F., Domanski, P.A., 2002. Comparative analysis of an automotive air conditioning systems operating with CO2 and R134a. Int. J. Refrigeration 25, 19–32.
Browne, M.W., Bansal, P.K., 2002. Transient simulation of vapour-compression packaged liquid chillers. Int. J. Refrigeration 25, 597–610.
Carrier Transicold, Ultra XT/Extra XT unit catalog, 2010a.
Carrier Transicold, Trailer and rail refrigeration-service parts list, 2010b.
Carrier Transicold, Truck refrigeration unit-operation and service, 2012.
Carrier Transicold, Vector 8600 MT unit catalog, 2013.
Casadei, A., Broda, R., Impact of vehicle weight reduction on fuel economy for various vehicle architectures, 2008.
Cho, H., Lee, H., Park, C., 2013. Performance characteristics of an automobile air conditioning system with internal heat exchanger using refrigerant R1234yf. Appl. Therm. Eng. 61, 563–569.
Defraeye, T., Cronjé, P., Verboven, P., Linus, U., Nicolai, B., 2015. Exploring ambient loading of citrus fruit into reefer containers for cooling during marine transport using computational fluid dynamics. Postharvest Biol. Technol. 108, 91–101.
Ding, G., 2007. Recent developments in simulation techniques for vapour-compression refrigeration systems. Int. J. Refrigeration 30, 1119–1133.
EPRI, Electric refrigerated container racks: technical analysis, 2010.
Fitzgerald, W.B., Howitt, O.J.A., Smith, I.J., Hume, A., 2011. Energy use of integral refrigerated containers in maritime transportation. Energy Policy 39, 1885–1896.
Galos, J., Sutcliffe, M., Cebon, D., Piecyk, M., Greening, P., 2015. Reducing the energy consumption of heavy goods vehicles through the application of lightweight trailers: fleet case studies. Transp. Res. Part D 41, 40–49.
Garthwaite, J., Smarter Trucking Saves Fuel Over the Long Haul. Inbound Logistics, 2012.
Haass, R., Dittmer, P., Veigt, M., Lütjen, M., 2015. Reducing food losses and carbon emission by using autonomous control – a simulation study of the intelligent container. Int. J. Prod. Econ. 164, 400–408.
Han, X.H., Li, P., Xu, Y.J., Zhang, Y.J., Wang, Q., Chen, G.M., 2013. Cycle performances of the mixture HFC-161 + HFC-134a as the substitution of HFC-134a in automotive air conditioning systems. Int. J. Refrigeration 36, 913–920.
Hermes, C.J.L., Melo, C., Knabben, F.T., Gonçalves, J.M., 2009. Prediction of the energy consumption of household refrigerators and freezers via steady-state simulation. Appl. Energy 86, 1311–1319.
Hill, H., Food miles: background and marketing, 2008.
International Energy Agency, CO2 emissions from fuel combustion, 2013.
James, S.J., James, C., Evans, J.A., 2006. Modelling of food transportation systems – a review. Int. J. Refrigeration 29, 947–957.
Jolly, P.G., Tso, C.P., Wong, Y.W., Ng, S.M., 2000. Simulation and measurement on the full-load performance of a refrigeration system in a shipping container. Int. J. Refrigeration 23, 112–126.
Joudi, K.A., Mohammed, A.S.K., Aljanabi, M.K., 2003. Experimental and computer performance study of an automotive air conditioning system with alternative refrigerants. Energy Convers. Manag. 44, 2959–2976.
Jul, M., 1985. Refrigeration and world food requirements. Int. J. Refrigeration 8, 6–9.
Koury, R.N.N., Machado, L., Ismail, K.A.R., 2001. Numerical simulation of a variable speed refrigeration system. Int. J. Refrigeration 24, 192–200.
Lee, G.H., Yoo, J.Y., 2000. Performance analysis and simulation of automobile air conditioning system. Int. J. Refrigeration 23, 243–254.
Li, B., Alleyne, A.G., 2010. A dynamic model of a vapor compression cycle with shut-down and start-up operations. Int. J. Refrigeration 33, 538–552.
Li, W., Liu, Z., Wang, Z., Dou, H., Wang, C., Li, J., 2016. Experimental and theoretical analysis of effects of equivalence ratio on mixture properties, combustion, thermal efficiency and exhaust emissions of a pilot-ignited NG engine at low loads. Fuel 171, 125–135.
Liang, N., Shao, S., Tian, C., Yan, Y., 2010. Dynamic simulation of variable capacity refrigeration systems under abnormal conditions. Appl. Therm. Eng. 30, 1205–1214.
Macagnan, M.H., Copetti, J.B., Souza, R.B., Reichert, R.K., Amaro, M., Analysis of the influence of refrigerant charge and compressor duty cycle in an automotive air conditioning system, in: 22nd Int. Congr. Mech. Eng. (COBEM 2013), 2013: pp. 6151–6161.
Moureh, J., Flick, D., 2004. Airflow pattern and temperature distribution in a typical refrigerated truck configuration loaded with pallets. Int. J. Refrigeration 27, 464–474.
Moureh, J., Tapsoba, S., Derens, E., Flick, D., 2009. Air velocity characteristics within vented pallets loaded in a refrigerated vehicle with and without air ducts. Int. J. Refrigeration 32, 220–234.
Natural Resources Canada, Fuel Efficiency Benchmarking in Canada's Trucking Industry, 2016.
Park, K.-J., Jung, D., 2007. Thermodynamic performance of HCFC22 alternative refrigerants for residential air-conditioning applications. Energy Build. 39, 675–680.
Rapalis, P., Skac, P., 2015. Research on the combustion, energy and emission parameters of diesel fuel and a biomass-to-liquid (BTL) fuel blend in a compression-ignition engine. Energy Convers. Manag. 106, 1109–1117.
Rodríguez-Bermejo, J., Barreiro, P., Robla, J.I., Ruiz-García, L., 2007. Thermal study of a transport container. J. Food Eng. 80, 517–527.
Shah, R.K., Sekulic, D.P., 2003. Fundamentals of Heat Exchanger Design. John Wiley & Sons.
Sørensen, K.K., Stoustrup, J., Bak, T., 2015. Adaptive MPC for a reefer container. Control Eng. Pract. 44, 55–64.
Spence, S.W.T., John, W., Doran, D.W., 2004. Art, design, construction and testing of an air-cycle refrigeration system for road transport. Int. J. Refrigeration 27, 503–510.
Tahil, W., How much lithium does a LiIon EV battery really need?, 2010.
Tassou, S.A., De-Lille, G., Ge, Y.T., 2009. Food transport refrigeration – approaches to reduce energy consumption and environmental impacts of road transport. Appl. Therm. Eng. 29, 1467–1477.
Tian, C., Li, X., 2005. Numerical simulation on performance band of automotive air conditioning system with a variable displacement compressor. Energy Convers. Manag. 46, 2718–2738.
Tso, C.P., Wong, Y.W., Jolly, P.G., Ng, S.M., 2001. A comparison of hot-gas by-pass and suction modulation method for partial load control in refrigerated shipping containers. Int. J. Refrigeration 24, 544–553.
UNEP, 2010 report on the refrigeration, air conditioning and heat pumps, 2010.
U.S. Energy Information Administration, How much carbon dioxide is produced by burning gasoline and diesel fuel? 2016.

Wang, F.Q., Maidment, G.G., Missenden, J.F., Tozer, R.M., 2007. A novel special distributed method for dynamic refrigeration system simulation. Int. J. Refrigeration 30, 887–903.

Wang, S., Gu, J., Dickson, T., Dexter, J., McGregor, I., 2005. Vapor quality and performance of an automotive air conditioning system. Exp. Therm. Fluid Sci. 30, 59–66.

WMO, UNEP, Climate change 2013; the physical science basis, 2013.

Wu, X., Hu, S., Mo, S., 2013. Carbon footprint model for evaluating the global warming impact of food transport refrigeration systems. J. Clean. Prod. 54, 115–124.

Yoo, S.Y., Lee, D.W., 2009. Experimental study on performance of automotive air conditioning system using R-152a refrigerant. Int. J. Automot. Technol. 10, 313–320.